

An Edge Analysis Based Blur Measure for Image Processing Applications

Yun-Chung Chung^{*}, Shyang-Lih Chang^{**}, Jung-Ming Wang^{*}, & Sei-Wang Chen^{*}

^{*} National Taiwan Normal University

^{**} Saint John's University

Abstract

In this project an edge-analysis-based non-parametric-image blur measure was proposed and evaluated. This measure is based on edge analysis and is suitable for various image-processing applications. The proposed measure for any edge point is obtained by combining the standard deviation of the edge gradient magnitude profile and the value of the edge gradient magnitude, using a weighted average. The standard deviation describes the width of the edge, and its edge gradient magnitude is also included to make the blur measure more reliable. Moreover, the value of the weight is related to image contrast and can be calculated directly from the image. Experiments in the natural scenes indicate that the proposed technique can effectively describe the blurriness of images in image-processing applications.

Keywords: blur measure, edge analysis, image contrast calculation

1. Interoduction

Blur measure - a measure of the sharpness or blurriness of edges in an image can be useful for a number of applications in image processing, such as checking the focus of a camera lens, helping to identify shadows (whose edges are often less sharp than object edges), the separation of variations in illumination from the reflectance of the objects in an image (known as intrinsic image extraction), and in-focus areas (or foreground) vs. out-of-focus (or background) areas in an image.

A novel method to determine the

blurriness of edges in a color RGB image is proposed in this paper. The method needs no user-supplied parameters like shapes and positions of objects or information about light sources. Nor is information about camera geometry and parameters required.

In the previous researches, Marziliano, Dufaux, Winkler, & Ebrahimi (2002) have proposed a no-reference perceptual blur metric (we prefer the term measure rather than *metric*), which they define in the spatial domain as the spread of the edges. (We briefly discuss and compare with their method in section II.)

In addition, Rooms, Pizurica, Philips (2002) have proposed a technique for measuring blur using wavelets. They calculate the sharpness of the sharpest edges in the image by computing the Lipschitz exponent for edges as a smoothness measure. The Lipschitz exponent (also known as the Hölder exponent) is a smoothness measure for a certain point. It is actually the result of how many times the image can be differentiable at a point. This measure is suitable for focus estimation without spatial domain processing to avoid noise effects. However, the estimated blur measure for a whole image may not be suitable for other applications.

Our proposed blur measure for an edge point is obtained by combining the standard deviation of the edge gradient magnitude profile and the value of the edge gradient magnitude using a weighted average. The

standard deviation describes the width of the edge, and the edge magnitude helps make the blur measure more reliable. The weight is calculated from the contrast of the input image and needs no manual inputs.

Experimental results covering intrinsic image extraction, image focusing, and in-focus vs. out-of-focus areas of an image are discussed in this paper. More applications of the proposed blur measure could also be investigated, such as shadow detection and removal, and benchmarking of the quality of image compression algorithms.

This paper is organized as the following descriptions. Our proposed non-parametric blur measure is described in section 2. Experimental results are discussed in section 3, and the concluding remarks are presented in section 4.

2. The Proposed Non-parametric Blur Measure

Fig. 1 presents a flowchart for the proposed non-parametric blur measure. Given an input color image $I(x, y)$, where x and y are the row and column coordinates, respectively, the gradient at any pixel location $p = (x, y)$ is calculated by applying the two-dimensional directional derivative.

$$\nabla I(x, y) = \begin{bmatrix} G_x \\ G_y \end{bmatrix} = \begin{bmatrix} \frac{\partial}{\partial x} I(x, y) \\ \frac{\partial}{\partial y} I(x, y) \end{bmatrix}. \quad (1)$$

The gradient magnitude (and two fast, decreasing accuracy approximations) at p can be obtained from G_x and G_y by (Gonzalez & Woods, 2002)

$$\begin{aligned} |\nabla I(x, y)| &= \sqrt{G_x^2 + G_y^2} \\ &\approx \frac{1}{2} [\max(G_x, G_y) + |G_x| + |G_y|] \approx |G_x| + |G_y|. \end{aligned} \quad (2)$$

Consider an edge point at $p = (x, y)$ defined as a local maximum of the edge gradient magnitude, and with the ζ -axis in the direction of the gradient. The origin of the ζ -axis is at the point of local maximum. Refer to Fig. 2. The edge width w is defined as the distance between the nearest local minima ($\zeta = m_l$ and $\zeta = m_r$) on each side of the maximum, i.e., $w = |m_l - m_r|$.

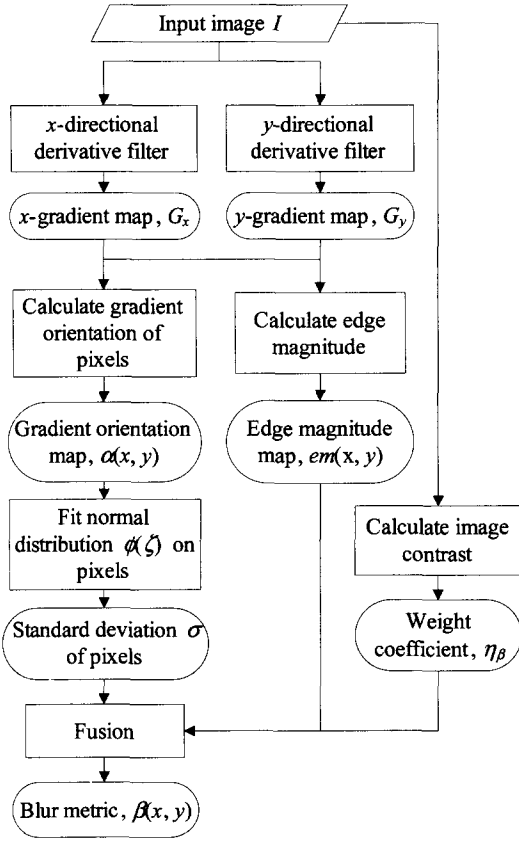


Figure 1. Flowchart of calculation of the proposed non-parametric blur measure

For comparison, the method of Marziliano, Dufaux, Winkler, & Ebrahimi (2002) calculated and averaged all the width values from the output of a vertical edge filter to define their blur metric for the whole image. Their method is quick, but, in some cases, can

be significantly affected by noise, as the example in Fig. 3 shows. The correct edge width should be w , while their calculated width was w' , the difference being caused obviously by noises around the edge pixel.

In our proposed method, local maximum points, $p' = (x', y')$, of the gradient magnitude of edges are used to denote the edge locations. The gradient orientation (direction of the ζ -axis) indicates the direction of the normal to the edge at p' with respect to the x -axis and is defined as $\alpha(x', y') = \text{atan2}(G_y, G_x)$, where we have used the atan2 function found in most programming languages since the result is in the interval from $-\pi$ to $+\pi$. We treat the edge gradient magnitude (across the edge) between $\zeta = m_l$ and $\zeta = m_r$ as a discrete probability distribution, with the mean at point p' , corresponding to $\zeta = 0$.

Let m_r be on the positive ζ -axis, and m_l be on negative ζ -axis, i.e., $m_r > 0$ and $m_l < 0$. Refer to Fig. 4. For this distribution, mathematically, the (spatial) variance is calculated as

$$\sigma^2(p') = \frac{1}{|m_r - m_l|} \sum_{\zeta=m_l}^{m_r} |\nabla I(\zeta)| \zeta^2. \quad (3)$$

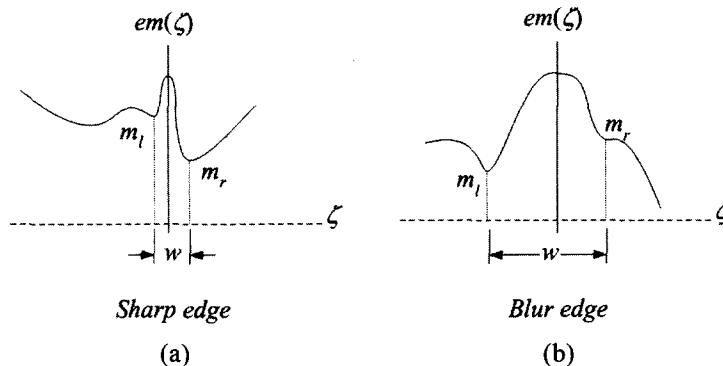


Figure 2. Gradient magnitude at an edge point $p = (x, y)$ in the direction ζ of the gradient. (a) sharp edge and (b) blurred edge.

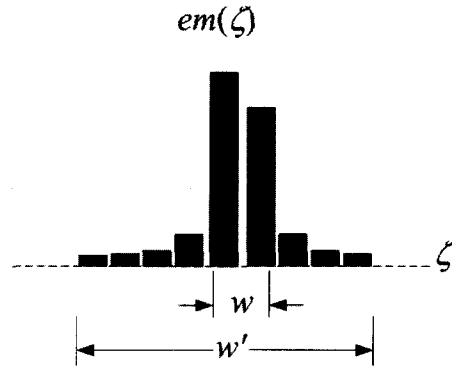


Figure 3. Illustration of bad estimation of edge width w as w'

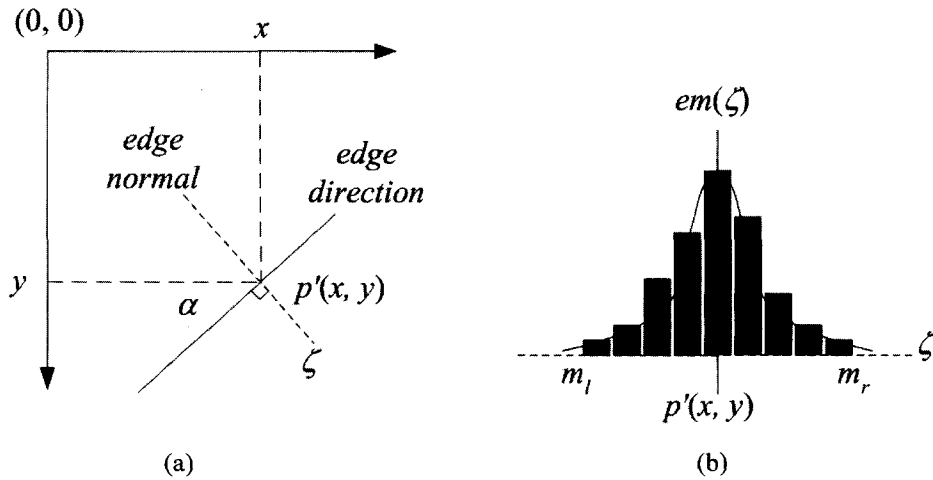


Figure 4. Illustration of the blur measure for an edge point $p'(x, y)$, (a) the edge point location, (b) fitting $em(\zeta)$ by normal distribution $\Phi(\zeta)$

(While this may be a scaled version of the variance, it does not matter, since in the next equation, it is divided by a normalizing term.) The blur measure $\beta(p')$ for an edge point p' is obtained by computing the weighted average of the standard deviation σ and the edge magnitude $|\nabla I(p')|$, and it is given by

$$\beta(p') = \eta_\beta \frac{\sigma(p')}{\sigma_{\max}} + (1 - \eta_\beta) \frac{|\nabla I(p')|}{|\nabla I(p')|_{\max}}, \quad (4)$$

where σ_{\max} and $|\nabla I(p')|_{\max}$ are normalization terms denoting the maximum values for all standard deviations and for all

edge gradient magnitudes.

In order to make the blur measure determined without any user-supplied parameters like shapes and positions of objects or information about light sources, the weight η_β is designed to be related to image contrast and is given by

$$\eta_\beta = \frac{1}{BC} \sum_{(x,y)} \sum_i \frac{|R_{MSR_i}(x,y)|}{\log I_i(x,y)}, \quad (5)$$

where B is the number of pixels in image $I(x, y)$ and C is the number of color bands. Since the color images that we are processing

are RGB images, we use $C = 3$, but it could be different for another color space; for example, for the CMYK color space, let $C = 4$.

Additionally, $I_i(x, y)$ is the i^{th} color band of image $I(x, y)$, and R_{MSR_i} is the i^{th} color component of the output of the Multiscale Retinex (MSR) algorithm (Jobson, Rahman, &

Woodell, 1997a), which is the combined weighted sum of N Single-scale Retinex [SSR] outputs (discussed below) (Jobson, Rahman, & Woodell, 1997b). The MSR output indicates the amount of enhancement needed for edge contrast. The i^{th} component of the MSR is given by

$$R_{MSR_i}(x, y) = \frac{1}{N} \sum_{n=1}^N [\log(I_i(x, y)) - \log(F_n(x, y) * I_i(x, y))] \quad (6)$$

where the symbol $*$ indicates convolution. $F_n(x, y)$ is a Gaussian smoothing filter and is calculated as $F_n(x, y) = Ke^{-(x^2+y^2)/c_n^2}$. Parameter c_n is the scale constant for the n^{th} scale, and K

is a normalizing constant such that $F_n(x, y)$ sums to 1. (Values of c_n are given from experiments and are discussed in the next section.)

3. Experimental Results

Sobel operators are commonly used as the filter to detect horizontal and vertical edges in digital images. Due to the discrete coordinate system used, the gradient directions α calculated from Sobel filters require a subpixel level correction to decrease the error in the

calculated angles (Ballard & Brown, 1982). To correct α , it is first reduced to the octant $[0, \pi/4)$. When α is in the range $\tan^{-1}(1/3)$ to $\pi/4$, the correction is given by (Ballard & Brown, 1982)

$$\alpha'(x, y) = \begin{cases} \alpha(x, y) & \text{if } 0 \leq \alpha \leq \tan^{-1}(1/3) \\ \tan^{-1} \left(\frac{7 \tan^2 \alpha + 6 \tan \alpha - 1}{-9 \tan^2 \alpha + 22 \tan \alpha - 1} \right) & \text{if } \tan^{-1}(1/3) < \alpha < (\pi/4). \end{cases} \quad (7)$$

Then the angle is restored to its proper octant. The difference between α and α' and the percent difference are shown in Fig. 5. The maximum error without correction is about 4.3%.

In addition, Jobson, Rahman, & Woodell (1997a) and Starck, Murtagh, Candes, & Donoho (2003) recommended that the number

of SSR scales of the MSR be three, and so we also used $N = 3$. Since this value gave good results, we did not bother experimenting with other values. Moreover, the Gaussian scale parameters c_n , ($n = 1, 2, 3$) in Jobson, Rahman, & Woodell (1997a) are suggested to take on the values 15, 80, and 250. These values are also employed in our experiments.

The error analysis of Sobel operators

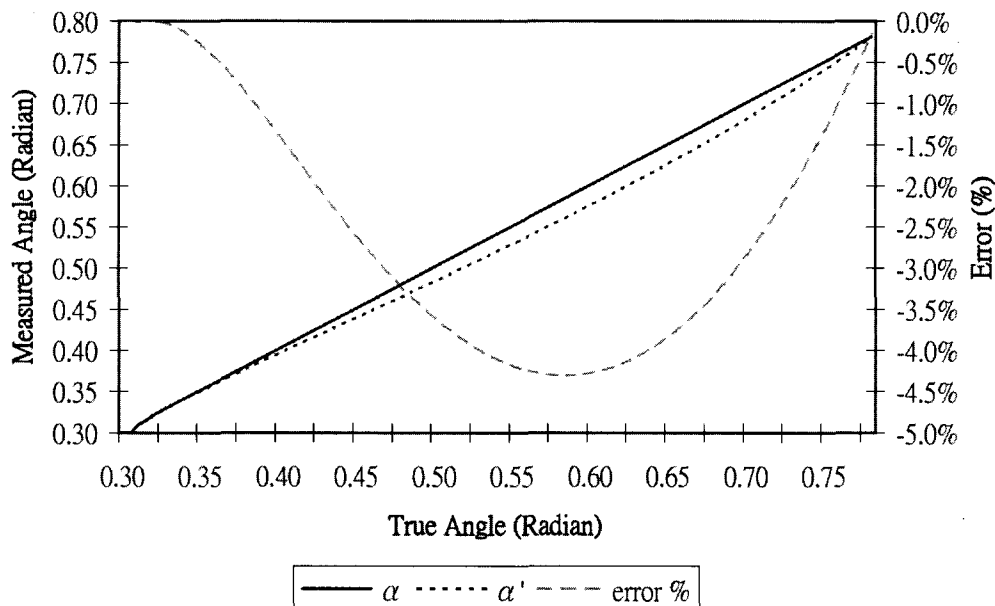


Figure 5. The difference of α (continuous line), α' (dotted line) and percent error (dashed line) of Sobel operators.

The following figures demonstrate some experimental results, in each figure; the input image is an RGB color image with a size of 320 by 240 pixels. Our program is written in the C language without any effort to optimize the speed and runs on a standard 2.4 GHz Pentium-based PC with 512 MB RAM. The computation of $\beta(x, y)$ took less than one second on the experiment PC.

Fig.6 shows an example image of the proposed blur measure. Applying vertical and horizontal derivative filters to the input image Fig. 6(a) produces the edge magnitude image Fig. 6(b), where blue indicates the vertical edge magnitude and green, the horizontal edge magnitude. From (5), weight η_β is calculated as 0.5772. The blur measure $\beta(x, y)$ for an edge point p' is obtained by averaging the standard deviation σ and the edge magnitude $|\nabla I(p')$

from (3). The blur measure is shown in Fig.6(c), where sharper edges correspond to higher intensities in the image.

There are many potential applications of the proposed measure. One is for the extraction of intrinsic images (i.e., reflectance and illumination images) from a single image. The blur measure provides important information about the scene illumination because edges of shadows tend to be blurred compared to object edges. With the proposed blur measure, the results of our previous study of the extraction of intrinsic images (Chung, Wang, Bailey, Chen, Chang, & Cherng, 2004) can be improved. Fig. 6(d) is the resulting improved reflectance image, comparing with the original reflectance image, Fig. 6(e) (Chung, Wang, Bailey, Chen, Chang, & Cherng, 2004), the details of the recovered reflectance image is

obviously better and this demonstrates that the proposed blur measure is effective, e.g., the utility pole in the left upper corner is better recovered in (d) than (e). Fig. 6(f) is the

improved illumination image, and the original illumination image is shown in Fig. 6(g) (Chung, Wang, Bailey, Chen, Chang, & Cherng, 2004).

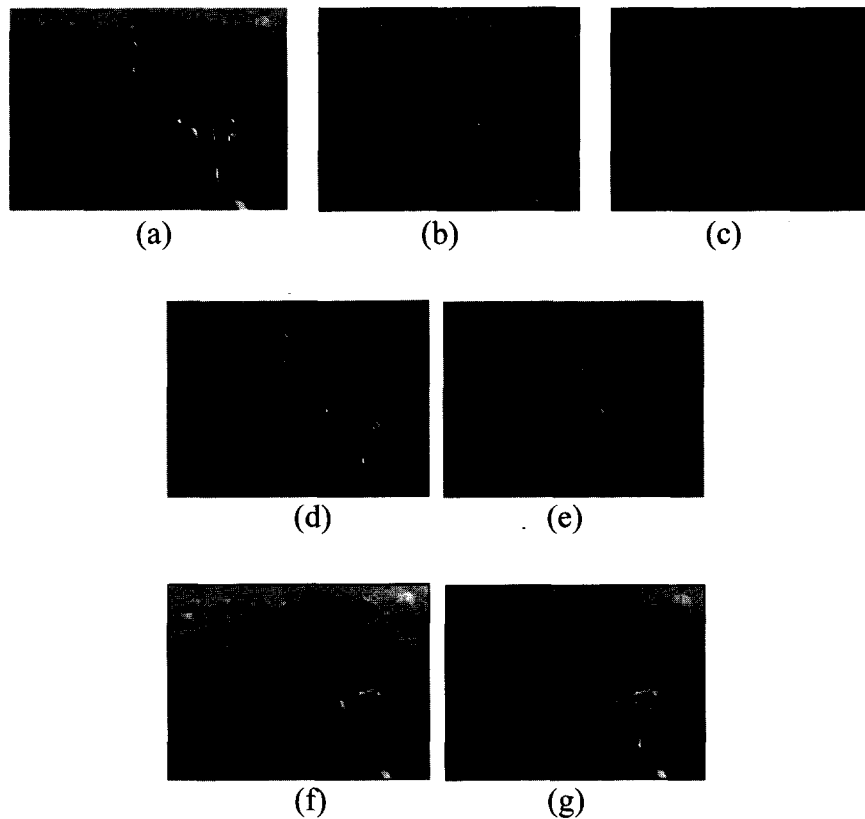


Figure 6. A blur measure example image. (a) input image, (b) edge magnitude image, blue is vertical edge, green is horizontal edge, (c) blur measure of edges; sharper edge has higher intensity in the image, (d) the improved reflectance image, (e) the original reflectance image, (f) the improved illumination image, and (g) the original illumination image.

Another example that is applicable to camera focusing is shown in Fig. 7. An in-focus image is shown in Fig. 7(a), and its edge magnitude image in Fig. 7(b). From (5), η_β is calculated as 0.6514. The blur measure image is shown in Fig. 7(c). An out-of-focus is shown in Fig. 7(d), and its edge magnitude

image in Fig. 7(e). A simple way of calculating a measure of focus F is given by

$$F = \sqrt{\frac{L \sum_{(x',y')} \beta(x',y')}{\sum_{(x',y')} |\nabla I(x',y')|}} \quad (8)$$

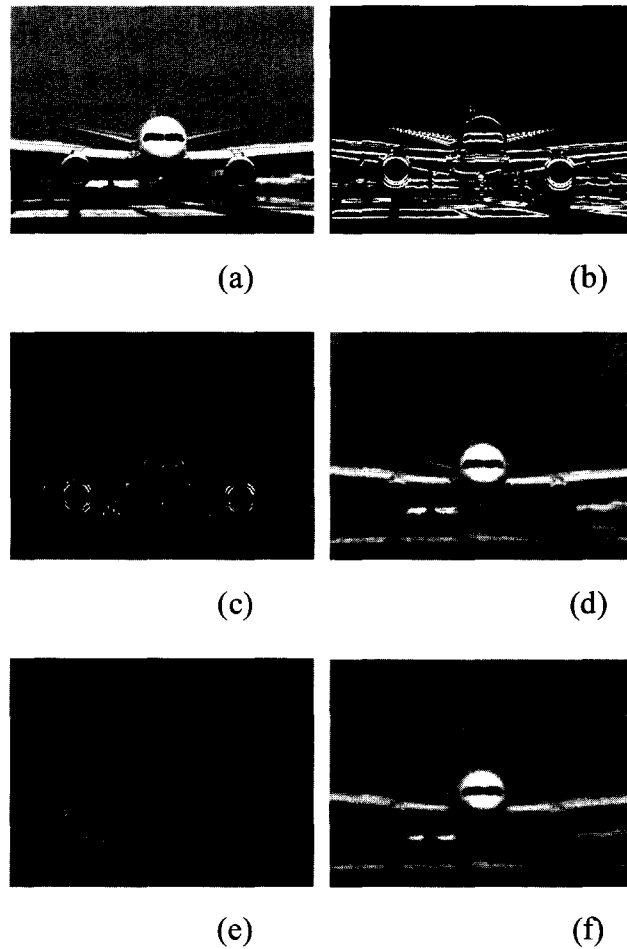


Figure 7. Another example of blur measure. (a) in-focus image, (b) edge magnitude image; blue is vertical edge, green is horizontal edge, (c) blur measure of edges; sharper edges have higher values, (d) out-of-focus image, (e) edge magnitude image of (d), and (f) an example more out-of-focus than (d)

L is a normalizing constant, where for a 256 level gradient image $|\nabla I(x, y)|$, $L = 255$ and, since $0 \leq \beta(x, y) \leq 1$, we have made the measure of focus $0 \leq F \leq 1$.

If the image is not correctly focused on the target, the blur measure can provide useful information to evaluate the image quality. For the images shown in Fig. 7(a) and (c) with correct focus, F is 0.564, Fig. 7 (d) and (e) are out of focus, and F is 0.459. A more blurred version of the image is shown in Fig. 7 (f) for

which F is 0.434.

Fig. 8 presents another example, with the input image in Fig. 8(a) and the edge magnitude image in Fig. 8(b). From (5), η_β is calculated as 0.6205. The blur measure of the edges is shown in Fig. 8(c). This example demonstrates that foreground (in-focus) and background (out-of-focus) can be distinguished using the blur measure. In this example, the birds in the foreground (near the camera) have sharp edges, while the background flowers and

plants (farther from the camera) are blurred.

More applications of the proposed blur measure could be investigated, such as shadow

detection and removal, and benchmarking of the quality of image compression algorithms, etc.

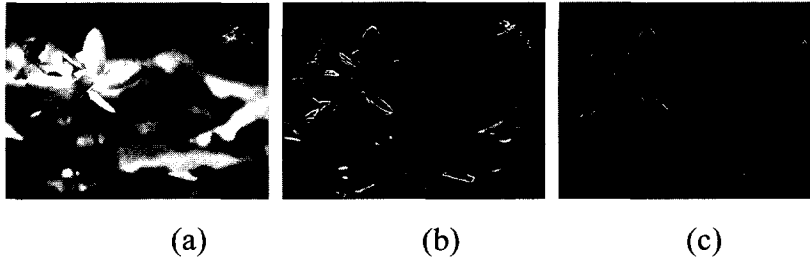


Figure 8. Another blur metric sample image. (a) the input image, (b) the edge magnitude image, blue: vertical edge, green: horizontal edge, (c) the blur metric of edges, sharper edge has higher intensity in the image.

4. Concluding Remarks

A novel technique for a non-parametric blur measure based on edge analysis was presented. The proposed blur measure $\beta(x, y)$ for any edge point $p' = (x', y')$ is obtained by a weighted average of the standard deviation of the edge magnitude profile around p' and the value of the edge gradient magnitude using a weighted average. The standard deviation plays an important role in effectively describing the edge width around p' , and its edge magnitude is also included to make the blur measure more reliable. Moreover, the value of the weight, which is based on image contrast information, is computed directly from the image.

The proposed blur was also tried with some applications, including the extraction of intrinsic images, camera focus, and foreground/ background classification. In addition, more applications of the proposed blur measure could be investigated, such as shadow detection and removal and benchmarking the quality of image compression algorithms, etc. In addition, the hardware implementation and reduction of this algorithm in the limited resources environments (e.g., digital cameras, cellular phones) can be one of the further researching topics.

References

- Ballard, D.H., & Brown, C.M. (1982). *Computer Vision*. New York: Prentice Hall.
- Chung, Y. C., Wang, J. M., Bailey, R. R., Chen, S. W., Chang, S. L., & Cherng, S. (2004, Aug.). *Physics-based Extraction of Intrinsic Images from a Single Image*. Paper presented at the 17th International Conference on Pattern Recognition, Cambridge, UK.
- Gonzalez, R. C., & Woods, R. E. (2002). *Digital Image Processing* (2nd ed.). New York: Prentice Hall.
- Jobson, D. J., Rahman, Z., & Woodell, G. A. (1997a). A multiscale retinex for bridging the gap between color images and the human observation of scenes. *IEEE Transactions on Image Processing*, 6(7), 965-976.
- Jobson, D. J., Rahman, Z., & Woodell, G. A. (1997b). Properties and performance of a center/surround retinex. *IEEE Transactions on Image Processing*, 6(3), 451-462.
- Marziliano, P., Dufaux, F., Winkler, S., & Ebrahimi, T., (2002, Sep.). *A no-reference perceptual blur metric*. Paper presented at the 2002 IEEE International Conference on Image Processing, N.Y.
- Rooms, F., Pizurica, A., & Philips, W. (2002, Jan). *Estimating image blur in the wavelet domain*. Paper presented at the meeting of the Fifth Asian Conference on Computer Vision (ACCV 2002), Melbourne, Australia.
- Starck, J.L., Murtagh, F., Candes, E. J., & Donoho, D.L. (2003). Gray and color image contrast enhancement by the curvelet transform. *IEEE Transactions on Image Processing*, 12(6), 706-717.

Acknowledgment

This work is supported in part by the National Science Council, Taiwan, Republic of China under contract NSC-92-2213-E-003-004.

Authors

鍾允中，國立臺灣師範大學資訊教育學系，研究生

Yun-Chung Chung is a Ph.D. student in the Department of Information and computer Education, NTNU, also a teacher in Taipei Municipal Shihlin Commercial High School, Taipei, Taiwan, R.O.C.

張祥利，聖約翰科技大學電子工程系，副教授

Shyang-Lih Chang is an Associate professor at the Department of Electronics Engineering, St. John's university, Taiwan, R.O.C.
E-mail:ali@mail.sju.edu.tw

王俊明，國立臺灣師範大學資訊教育學系，研究生

Jung-Ming Wang is a student in the Department of Information and Computer Education, National Taiwan Normal University.

陳世旺，國立臺灣師範大學資訊工程學系，教授

Sei-Wan Chen is a Professor at the Graduate Institute of Computer Science and Information Engineering at National Taiwan Normal University, Taipei, R.O.C.

收稿日期：93.09.14

修正日期：93.10.26

接受日期：93.12.01

基於邊緣分析之模糊測量標準— 於影像處理之應用

鍾允中
國立臺灣師範大學

張祥利
聖約翰科技大學

王俊明 陳世旺
國立臺灣師範大學

摘 要

本論文中提出一個新的基於邊緣分析之模糊測量標準。本項模糊測量標準是基於邊緣分析的基礎而訂立，此模糊測量標準適用於各種不同之影像處理應用。本論文所提出的方法針對所有邊緣點分析，以加權的方式結合邊緣梯度變異量資訊以及邊緣梯度強度資訊，定義出本項模糊測量標準。邊緣梯度變異量資訊描述了邊緣的寬度資訊，而邊緣梯度強度資訊則讓邊緣資訊更加的可靠。此外，加權的值並不需要人工輸入，而是直接由輸入影像的對比資訊自動決定。由實驗的結果中顯示，本論文所提出的方法在許多影像處理應用上都有良好的結果。

關鍵字：模糊測量、標準邊緣分析、影像對比分析